NASA TN D-1598

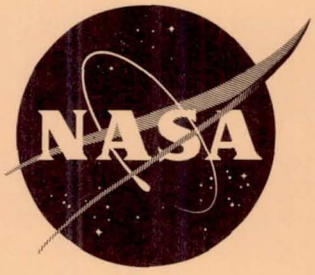


# TECHNICAL NOTE

D-1598

## DESIGN, OPERATION, AND TESTING CAPABILITIES OF THE LANGLEY 11-INCH CERAMIC-HEATED TUNNEL

By Otto F. Trout, Jr.

Langley Research Center
Langley Station, Hampton, Va.

NATIONAL AERONAUTICS AND SPACE ADMINISTRATION
WASHINGTON

February 1963

NATIONAL AERONAUTICS AND SPACE ADMINISTRATION

TECHNICAL NOTE D-1598

# DESIGN, OPERATION, AND TESTING CAPABILITIES OF THE LANGLEY 11-INCH CERAMIC-HEATED TUNNEL

By Otto F. Trout, Jr.

## SUMMARY

Supersonic air jets and tunnels, suitable for performing materials research, aerodynamic testing, and heat-transfer studies, have been designed and built and coupled with a ceramic heat exchanger which operates up to 4,500° R. Details for the ceramic heat exchangers, water-cooled supersonic nozzles, premixed-gas combustion equipment, and control systems for these facilities have been worked out and have been applied to existing facilities.

The present paper presents a general discussion of the important design problems applicable to ceramic-heated air tunnels and includes flow conditions, heat transfer, and construction details. The Langley 11-inch ceramic-heated tunnel, which can be used either as a Mach 4 free jet with a 4-inch-diameter nozzle or as a Mach 6 closed tunnel which provides a 10.5-inch-diameter flow, is discussed as a typical facility which utilizes a ceramic pebble-bed heat exchanger.

## INTRODUCTION

Aerodynamic heating from flight conditions at hypersonic speeds has presented new problems in aerodynamics, structures, and materials. In order to obtain economical solutions to some of the problems, higher stagnation temperature ground test facilities are needed to study aerodynamic heating at hypersonic speeds, to study imperfect gas effects at high temperatures, and to study the reaction of ablative and heat-sink materials in high-temperature, high-velocity air. The NASA has therefore made a study of high-temperature testing facilities such as electric arc heaters, electric induction heaters, shock tubes, combustion tunnels, rocket jets, and high-temperature ceramic heat exchangers. Inasmuch as oxidation is a major problem in materials research, facilities producing high-temperature air in contrast to rocket-jet facilities were of particular interest. One significant phase of this work has been the development of ceramic heat exchangers capable of producing temperatures of approximately 4,500° R. This type of heat exchanger has been utilized at moderate temperatures in blast-furnace regenerators, packed beds, and pebble-bed heat exchangers for heating gases; some of these facilities are described in references 1 through 4. A considerable amount of information is available on their operation.

Early work on adapting such a ceramic heat exchanger to aerodynamic testing was done at the University of Minnesota (ref. 5). Additional work was done at Brooklyn Polytechnic Institute with a facility having a pebble-bed heat exchanger constructed of alumina and capable of producing bed temperatures of 3,500° R (ref. 6).

L-58-1494

Figure 1.- Langley 11-inch ceramic-heated tunnel.

At the time design was started on the facility discussed herein, many problems existed in extending the temperature capabilities of ceramic-heated air facilities. Some of these problems were associated with the containment of a 4,500° R pebble bed in a pressure vessel: the ability of the ceramics to withstand thermal shock, pressurization, and depressurization; the problem of economically heating the ceramics without contamination or damage; and the incorporation of the various components into a successfully operating facility.

These problems led to the construction at the Langley Research Center of a small ceramic heat exchanger which utilizes zirconia ceramics. This heat exchanger provided air for a Mach 2 aerodynamic testing facility at mass-flow rates up to 0.3 lb/sec as described in references 7 and 8. The successful operation of this facility led to the construction of a larger facility (fig. 1) which is capable of delivering airflow up to 15 lb/sec up to 1,200 lb/sq in. stagnation pressure, with heat-exchanger temperatures up to 4,500° R, providing flow for either a Mach 4 free jet (described briefly in ref. 9) or a Mach 6 enclosed jet system.

The facility, its operation, and its performance characteristics are described herein. Also included is a brief discussion of some of the approaches investigated in the design of the heat exchanger, the water-cooled nozzles, and the pebble-bed heating system.

## SYMBOLS

| | |
|---|---|
| A | area |
| D | diameter |
| f | friction factor |

| | |
|---|---|
| $F_f$ | friction-factor factor |
| g | gravitational constant |
| h | heat-transfer coefficient |
| k | thermal conductivity |
| K | constant |
| $l$ | length or depth of bed |
| M | Mach number |
| R | Reynolds number |
| $N_{Pr}$ | Prandtl number |
| P | wetted perimeter |
| p | pressure |
| q | heat-transfer rate |
| Q | heat-transfer resistance coefficient = 1/h |
| t | thickness |
| T | temperature, degrees Fahrenheit or degrees Rankine, as indicated |
| V | velocity |
| E | modulus of elasticity |
| $\mu$ | Poisson's ratio |
| $\nu$ | coefficient of viscosity |
| $\eta$ | coefficient of thermal expansion |
| $\sigma$ | stress |
| $\rho$ | density |

Subscripts:

| | |
|---|---|
| aw | adiabatic wall |
| b | bulk water conditions |
| e | effective |

| | |
|---|---|
| g | gas |
| L | liquid |
| s | sphere |
| t | thermal |
| w | wall |
| $\infty$ | free stream |

## DESCRIPTION AND OPERATION OF APPARATUS

### General Description

A diagram for a ceramic-heated air jet facility is presented in figure 2. Such a unit consists of a pressure vessel lined with a refractory and containing, in the center, a bed of randomly packed pebbles or spheres. For the heating cycle, a burner is provided which heats the pebble bed by forcing the products of combustion downward through the pebble bed until the desired temperature distribution is attained. For the testing cycle, the burner is closed off, and air is passed upward through the pebble bed and exhausted through a water-cooled nozzle at the top of the pressure vessel. A quartz window in the side of the pressure vessel permitted temperature readings to be taken at the top of the pebble bed.

As a specific example figure 1 shows the Langley ceramic heat exchanger with a test house on top for mounting the Mach 4 free-jet nozzle or the Mach 6 nozzle diffuser system. Used with the Mach 6 nozzle, this facility is known as the 11-inch ceramic-heated tunnel. The heat exchanger shown in the general diagram in figure 2 consists of a 54-inch-diameter steel tank 30 feet high lined with 12 inches of refractory and containing a 28-inch-diameter bed of 3/8-inch-diameter spheres, randomly packed 20 feet deep.

Figure 3 presents a diagram of the Mach 6 nozzle and the diffuser system which is used interchangeably with the Mach 4 free-jet nozzle.

### Heat-Exchanger Design

Choice of materials.- In choosing ceramics for use in the heat exchanger, consideration must be given to the fact that air is used as the test medium, and that it is desirable to choose a ceramic which will produce the least reaction with air at the highest possible stagnation pressures and temperatures. A study was made of the properties of commercially available, high-temperature ceramics which might be used in the construction of the heat exchanger. Inasmuch as it was desired to build a heat exchanger which would permit operation at temperatures up to 4,560° R for heating air, the following properties were considered: mechanical strength as a function of temperature; reaction with air and other materials;

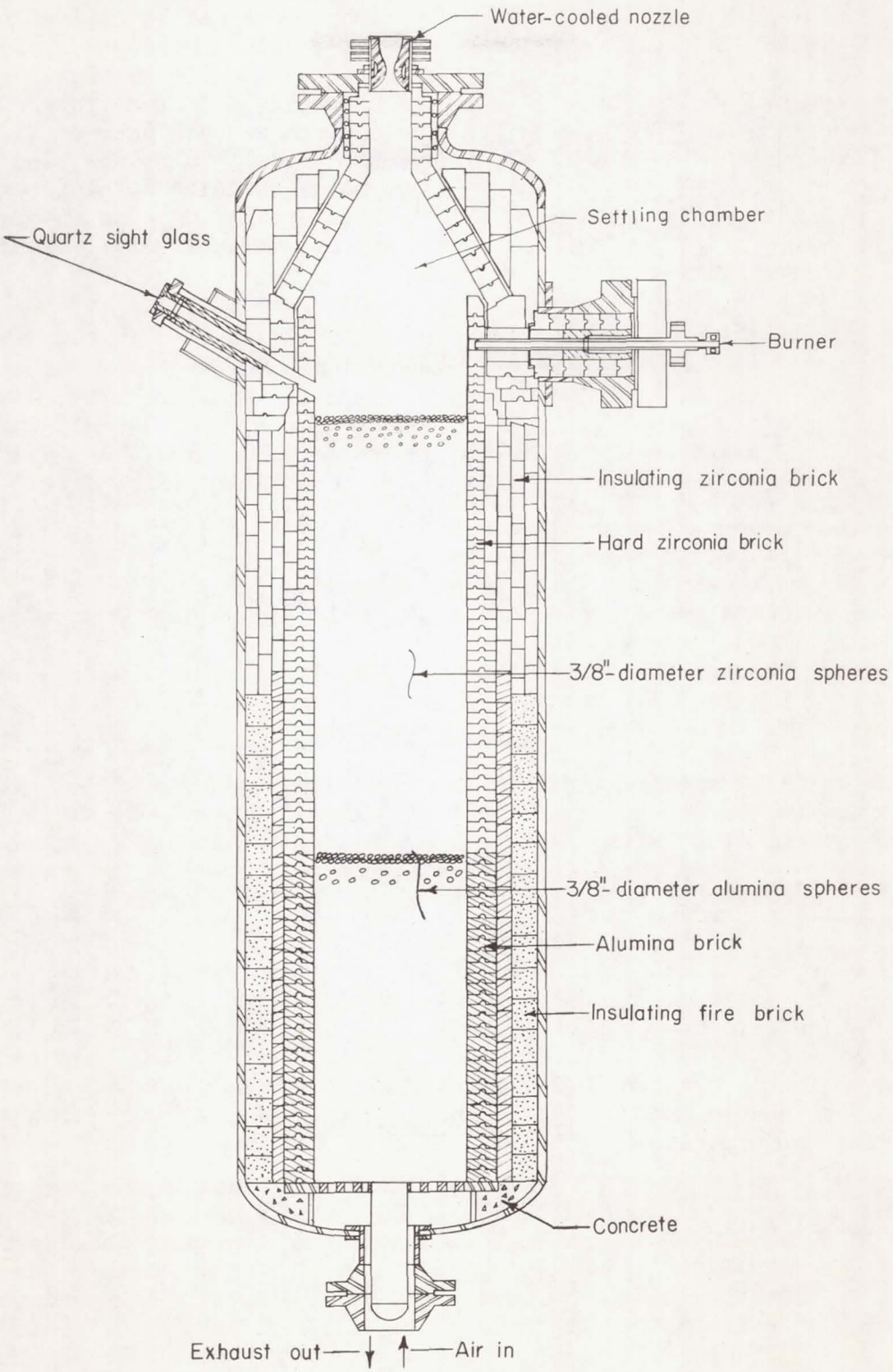


Figure 2.- Ceramic-heated tunnel and water-cooled nozzle.

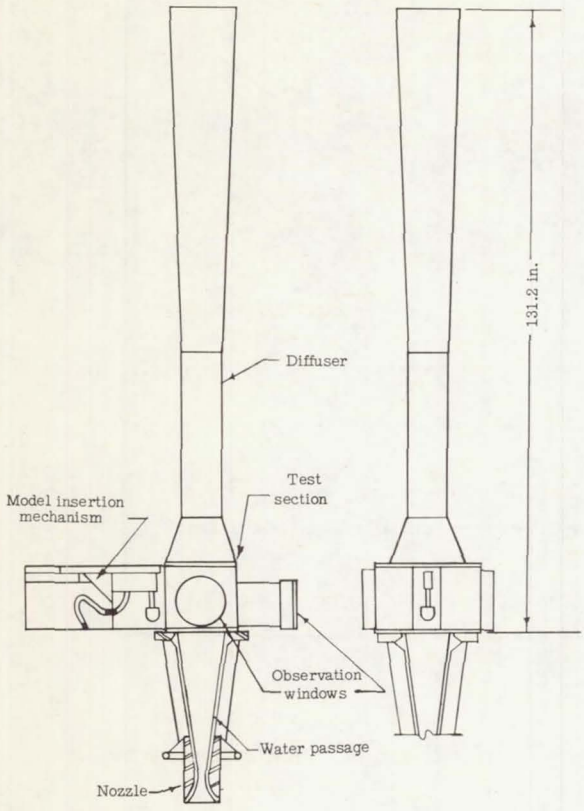


Figure 3.- Mach 6 nozzle and test section.

density, thermal conductivity; heat capacity; abrasion resistance; and thermal shock resistance upon heating and cooling; availability; and health hazards. Only the oxides were considered since other refractories such as carbides, nitrides, silicides, borides, sulphides, and the refractory metals oxidize at high temperatures in air. A detailed discussion of the various oxides is available in references 10 and 11.

Zirconia ($ZrO_2$) with a melting point of 5,330° R was used in the heat exchanger rather than thoria ($ThO_2$) or beryllia (BeO) (because of their potential health hazards and high cost), or magnesia (MgO) (because of its lower density and higher vapor pressure), or alumina ($Al_2O_3$) (because of its lower melting point). Zirconia appeared to be the most promising commercially available refractory for use in a heat exchanger which produced temperatures up to 4,500° R. However, zirconia does have several disadvantages: its surface is less resistant to abrasion than alumina; it may revert to zirconium carbide at high temperatures in a carbonaceous reducing atmosphere, and in the pure state, it passes through a crystalline inversion between 2,000° and 2,900° R.

The commercial zirconia originally used in the heat exchanger was the partially stabilized product chosen for its high resistance to thermal shock. Successful operation of the heat exchanger was obtained with the partially stabilized product; however, decomposition occurred in certain regions of the heater lining with time. It was found that the partially stabilized zirconia in sections of the unit which were heated above 2,000° R, but not above 2,900° R, lost strength completely after repeated cycling. However, the same product retained its strength when heated above 2,900° R. A series of controlled experiments in a laboratory kiln were made to define the nature of the problem. They showed that the problem was associated with crystalline inversion.

Figure 4 presents a diagram of the linear expansion of zirconia as a function of temperature during heating and cooling, as presented in reference 12. Pure zirconia has a monoclinic crystalline structure at lower temperatures and undergoes a sudden change to tetragonal form with an accompanying decrease in volume, beginning at 2,300° R; upon cooling it reverts to the monoclinic form with a subsequent increase in volume. The bond between the crystals breaks down and thereby reduces the strength of the ceramic body to nearly zero when nonstabilized zirconia is cycled through this inversion region.

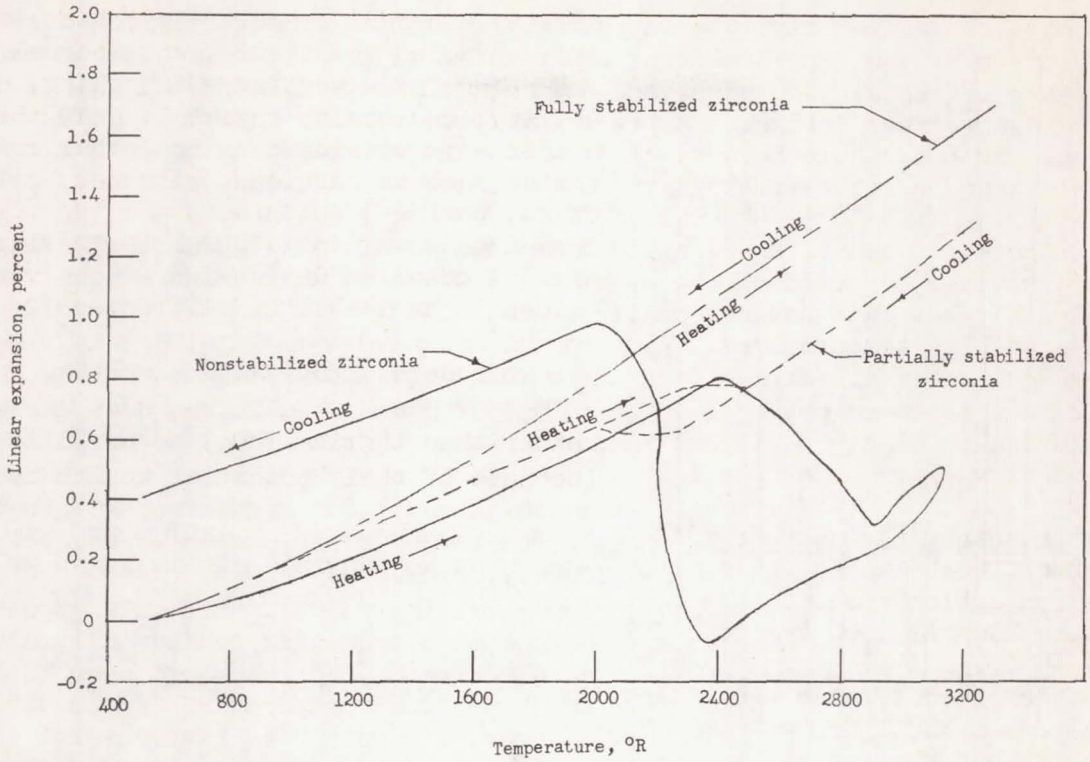


Figure 4.- Linear expansion as a function of temperature for zirconia. From reference 12.

The partially stabilized zirconia, produced by adding 5 percent to 6 percent calcium oxide (CaO) to give a predominantly cubic structure, undergoes only a small volumetric change in cycling through the inversion region. However, tests show that the material breaks down after being repeatedly cycled (approximately 50 times) from 1,900° R to 2,500° R. Tests were also run on fully stabilized zirconia; it did not break down under the same conditions. Fully stabilized zirconia, made by adding 10 percent to 12 percent calcium oxide, having a fully cubic crystalline structure retains its crystal form on heating and cooling and was found to retain its strength. It is also known that this product is less resistant to thermal shock than the partially stabilized product. Fully stabilized (cubic) zirconia is now used in portions of the heat-exchanger wall which are not heated above 2,900° R where it appears to cycle satisfactorily even though it is less resistant to thermal shock.

The load-bearing capability of zirconia decreases rapidly with temperature; at 3,960° R, its compressive strength is about 45 lb/sq in. (ref. 12). In the absence of available data, measurements were made at Langley Research Center of the strength of zirconia at 4,460° R. At this temperature, zirconia has a strength of 7 lb/sq in.

In order to prevent loading the ceramics beyond their capabilities at any place in the pebble bed, the pebble bed was designed for a decreasing temperature through the bed, with 4,560° R as the maximum temperature at the top of the bed and 1,460° R as the maximum temperature at the bottom of the bed.

Although commercial zirconia is fairly resistant to thermal shock, care must be exercised to prevent rapid heating and cooling of the ceramics. Large ceramic shapes, sharp overhanging corners, and areas of shear were avoided in the design. The heat exchanger was designed to prevent passage of air through the brickwork (thus bypassing the pebble bed) by staggering the joints, avoiding open spaces, and by inserting cement barriers between the layers of brick.

Other ceramics can be used in the lower temperature sections of the heat exchanger; however, care should be exercised in their choice since solid-state reactions can take place between unlike ceramics which completely alter their properties at high temperatures. Alumina ceramics were used in zones of the heat exchanger and the outer brick lining where the temperature does not exceed 2,460° R. Reference 10 presents a phase diagram for the alumina-zirconia reaction. Alumina is highly resistant to abrasion; therefore, very little of it will sift or be blown into other sections of the heat exchanger.

Heat transfer through ceramics.- The main heat-transfer considerations in the design of the heat exchanger were the heat transfer through the ceramic lining from the combustion gases to the pebbles, and from the pebbles to the air during the heating and blowdown cycles.

In order to determine the lining thickness required to keep the steel pressure-vessel shell below 1,060° R under peak temperature conditions, steady-state conditions were assumed, and shell temperature was computed by the method of total resistance. Steady-state heat conduction through walls of unlike solids may be calculated by dividing the total temperature drop by the total resistance, which is the sum of the individual resistances. The heat transfer then is

$$q = \frac{\Delta T}{\frac{1}{h_1} + \frac{1}{h_2} + \frac{1}{h_3} + \frac{1}{h_4} + \frac{1}{h_5}}$$

where subscripts 1, 2, and 3 are the successive layers of ceramics, 4 is the pressure-vessel shell, $h_5$ is the convective heat-transfer coefficient of the outside wall to the air, and $\Delta T$ is the temperature difference between the inside wall and the outside cooling air.

Design of the ceramic walls was based on conditions at the top of the bed where maximum heat transfer occurs. The same thickness of insulation was used in the remainder of the pressure vessel to prevent excessive heat loss. Basing the design of the heat exchanger on steady-state conditions for maximum operating temperature gave conservative, satisfactory engineering results. In actual practice the maximum bed temperature of 4,560° R is seldom maintained for more than 2 hours. Measurements show that under this condition, the shell temperature does not exceed 970° R.

Heat transfer through the packed bed of spherical particles for conditions of stagnant interstitial gas, that is, no flow through the heat exchanger, was calculated by conventional methods (ref. 13), to determine the order of heat fluxes during idling conditions.

The capabilities of the pebble bed as a heat exchanger with flowing gases were investigated by a computational procedure which considered the heat conduction through the insulating side walls and utilized theoretical and experimental heat-transfer information on pebble-bed heaters from references 13 and 14.

Pressure drop through pebble bed.- Pressure drop across the packed bed is an important factor in the design of a pebble-bed heat exchanger. When the pressure drop multiplied by the cross-sectional area becomes equal to the weight of the bed, a partial fluidization begins to take place.

Several methods which have been used to calculate differential pressure drop through packed beds are presented in references 1, 14, and 15. The methods in reference 15 give satisfactory engineering answers over a wide range of conditions when used with previously determined experimental friction factors. Since a temperature differential is maintained through the bed, differential pressure over increments of the bed is calculated by

$$-\Delta p = \frac{f(F_f)\,l V^2 \rho}{2 g D_s}$$

where

$D_s$ diameter of spheres

$V$ effective velocity based on empty cross-sectional area

$\rho$ density of gas

$l$ length of pebble bed

$-\Delta p$ pressure drop due to friction

In the absence of available data on zirconia spheres, values of friction-factor factor $F_f$ and friction factor $f$ for alumina spheres of comparable size, tabulated in reference 1, were used in the computations to determine pressure drop through any section of the bed.

Figure 5 presents measured pressure drop compared with theory across the pebble bed of the 11-inch ceramic-heated tunnel during a typical run. Stagnation pressure is also plotted. The pressure drop during the pressurization period must be closely controlled, since it may be several times the value of steady-state operation. In actual operation, the allowable pressure drop is limited to 75 percent of that required to lift the bed.

Method of heating the bed.- Because of the size of the bed and the temperatures involved, a combustion heater was the most practical for heating the bed. The combustion system must heat the bed under controlled temperatures and heating rates in order to obtain the desired temperature distribution, must not contaminate the ceramics, must be controllable over the entire operating range, and must

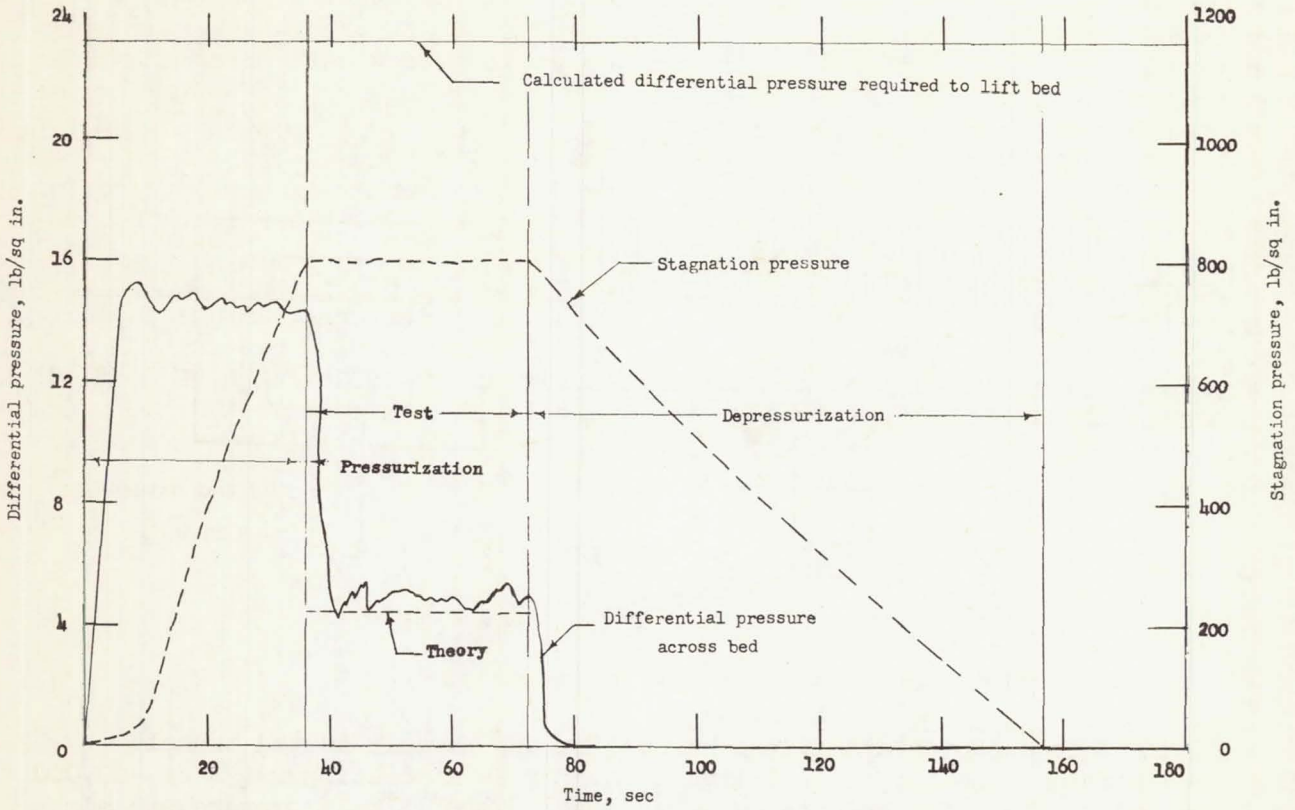


Figure 5.- Differential pressure and stagnation pressure as a function of time for a typical test run for the 11-inch ceramic-heated tunnel.

produce complete combustion in a very small space. After a study of the requirements and experimental work with burner types which use both gas and oil (see ref. 1), a gas-fired premixed burner was chosen for use in this system. Propane was chosen as the fuel because it was readily available and easy to meter and control. Oxygen enrichment of the combustion air was necessary to heat the ceramics to 4,560° R inasmuch as the propane-air combustion temperature is several hundred degrees less than 4,560° R.

Figure 6 presents a diagram of the fuel-air mixing device, or burner, used with the ceramic-heated facility. Propane, air, and oxygen are mixed together in the center tube of the burner and are injected into the settling chamber (fig. 2) above the pebble bed where combustion takes place. Velocity of the gas mixture in the inner tube of the burner is sufficient to prevent flashback at all firing rates and fuel-air-oxygen mixtures used in the operation. Flame velocity, combustion temperatures, and gaseous diffusion rates of propane-air-oxygen mixtures can be calculated by methods presented in reference 16.

Circulation of water through the outer jacket of the burner prevents overheating of the metal parts where they extend through the heated ceramic wall (fig. 2). Premixing of propane-air and oxygen in the inner tube of the burner produces a clean, carbon-free, continuous, low-luminosity flame at all operating conditions.

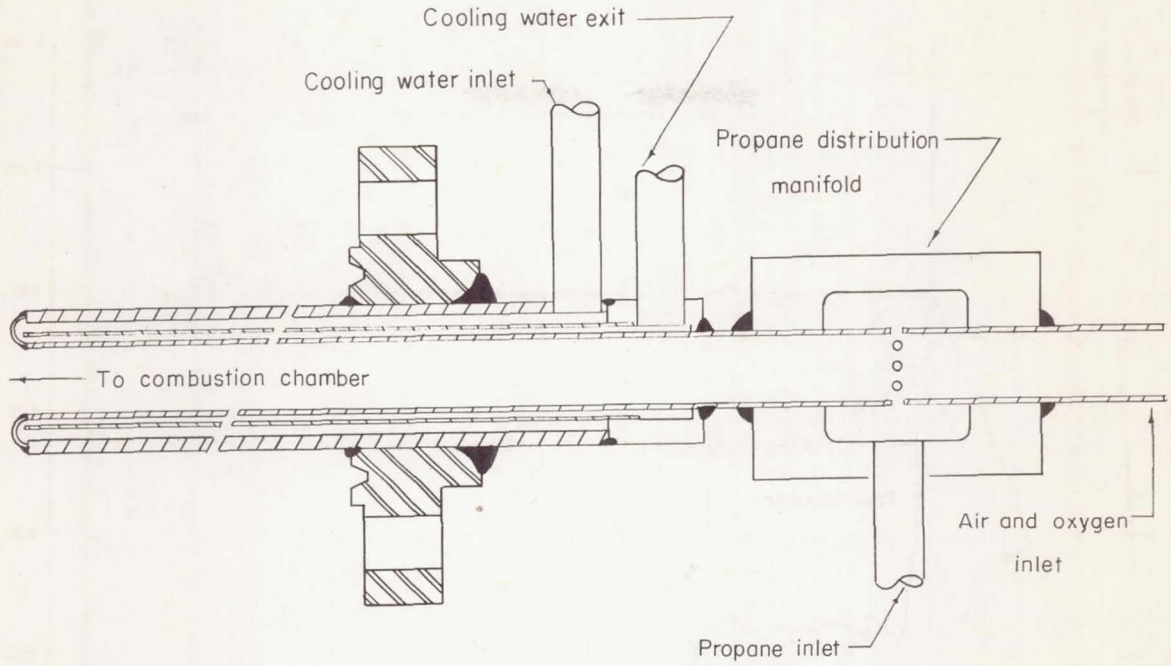


Figure 6.- Diagram of burner for heating pebble bed.

Figure 7 is a photograph of the burner for the ceramic-heated tunnel described herein. The burner is designed to operate at heating rates of 400,000 to 2,000,000 Btu/hr. For bed temperatures up to 3,600° R only propane and air are used; for higher temperatures, commercial oxygen is used to obtain higher flame temperatures. At 4,500° R 60 percent of the required oxygen is supplied by commercial oxygen, and 40 percent is supplied by air. Higher oxygen-air ratios are not used since 4,500° R is considered the maximum safe operating temperature for this facility. In order to maintain an oxidizing atmosphere which is necessary for complete combustion of the fuel, oxygen, 10 percent in excess of that required for a stoichiometric mixture, is used.

When the ceramics are cold, ignition is accomplished with a gas-fired igniter. Above 1,900° R, bed-temperature ignition is spontaneous when the fuel-air flow is begun.

Figure 8 presents a diagram of the burner control system. Fuel-air and oxygen rates are regulated by means of manually operated valves while the rates

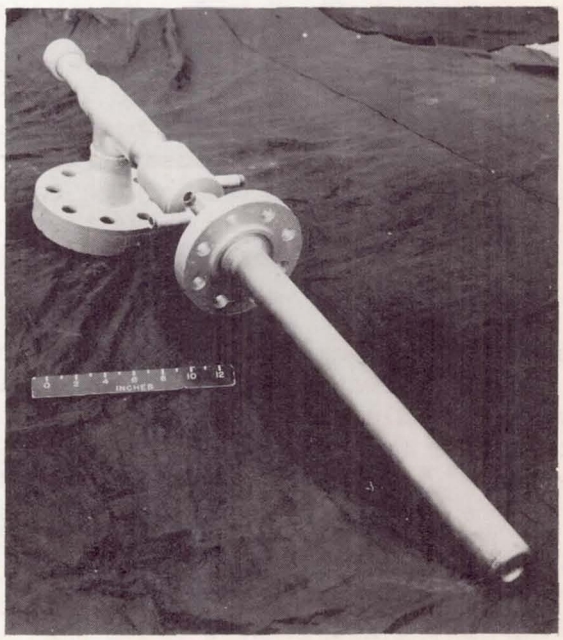

L-60-1218

Figure 7.- Photograph of burner for heating pebble bed.

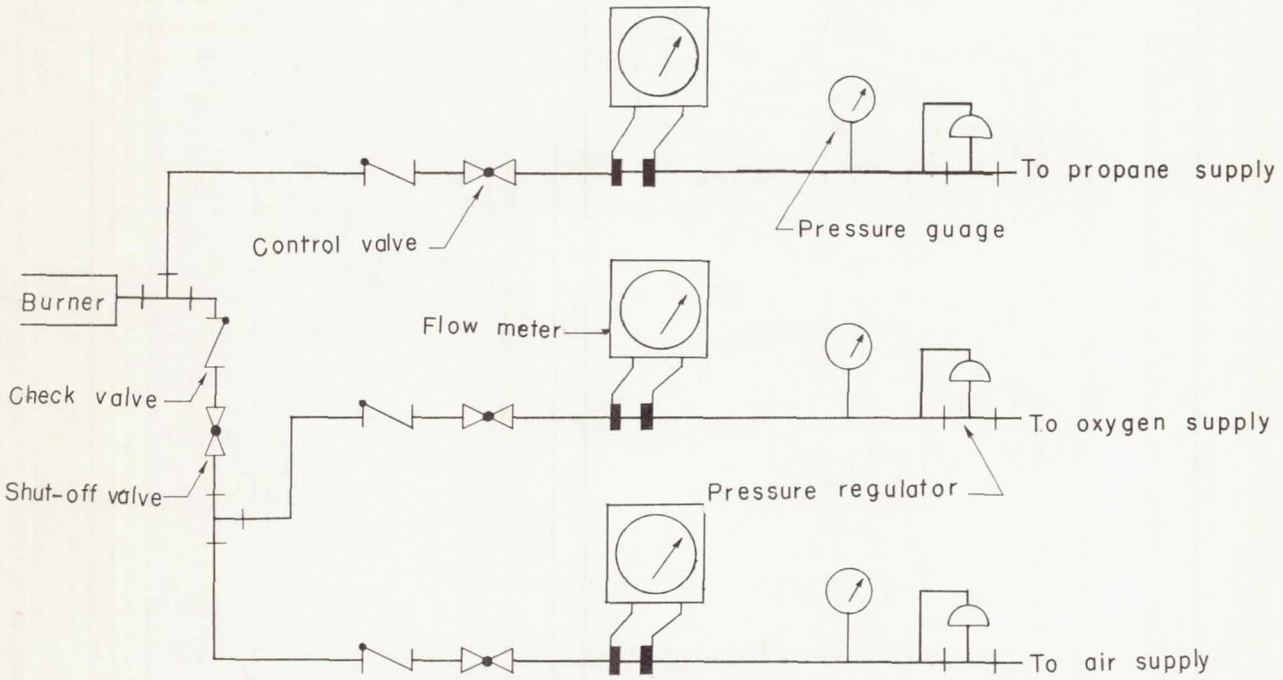


Figure 8.- Diagram of burner control system for ceramic heat exchanger.

of each are measured by manometers connected to low-pressure-drop, sharp-edged-orifice meters. Fuel and oxidizer rates are accurately controlled during the heating cycle.

The premixed gas-fired combustion system has proved highly satisfactory for heating the heat exchanger throughout its range of operation.

## Nozzle Design

Mach 4 nozzle.- Figure 9 presents a diagram of the Mach 4 water-cooled nozzle with a tabulation of the ordinates downstream of the throat, and figure 10 presents a photograph of the nozzle. The nozzle has an exit diameter of 4 inches and exhausts to the atmosphere. Ordinates for the nozzle, designed for a minimum length, were determined by methods presented in reference 17.

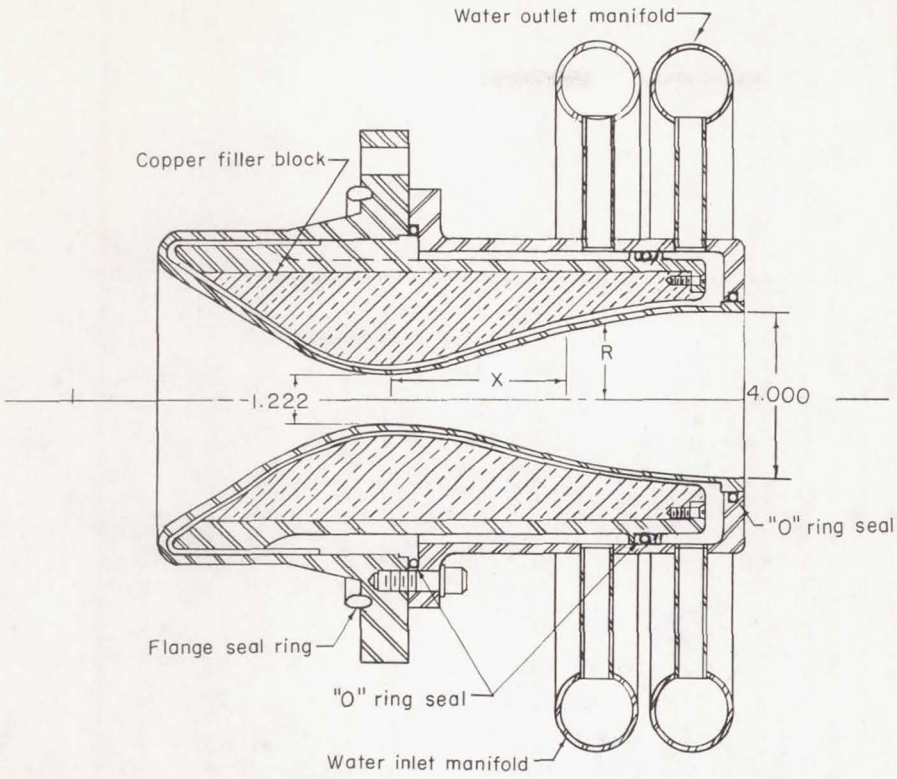


Nozzle ordinates downstream of throat.

| X | R |
|---|---|
| 0.000 | 0.611 |
| 0.250 | 0.704 |
| 0.500 | 0.786 |
| 0.750 | 0.871 |
| 1.000 | 0.941 |
| 1.250 | 1.013 |
| 1.500 | 1.082 |
| 1.750 | 1.150 |
| 2.000 | 1.213 |
| 2.250 | 1.274 |
| 2.500 | 1.333 |
| 3.000 | 1.441 |
| 3.500 | 1.537 |
| 4.000 | 1.620 |
| 4.500 | 1.691 |
| 5.000 | 1.756 |
| 5.500 | 1.812 |
| 6.000 | 1.860 |
| 6.500 | 1.901 |
| 7.000 | 1.933 |
| 7.500 | 1.961 |
| 8.000 | 1.984 |
| 8.500 | 2.000 |
| 8.5376 | 2.001 |

Figure 9.- Diagram of water-cooled Mach 4 nozzle. Dimensions are in inches.

The inner wall and throat section of the nozzle are constructed of T-1 high-strength alloy steel. The wall thickness at the throat is 0.062 inch. A solid copper filler block (fig. 9) directs the cooling water along the inner wall of the nozzle and also acts as a heat sink in case of failure of the nozzle wall which would prevent rapid opening of the nozzle throat.

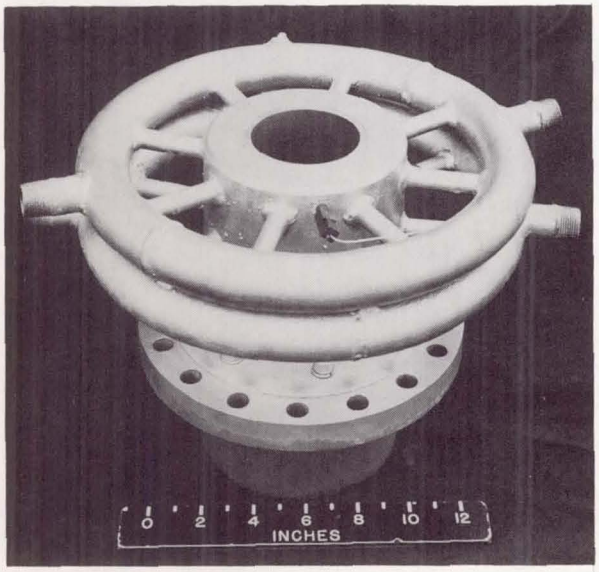


L-60-1222

Figure 10.- Photograph of Mach 4 water-cooled nozzle.

Figure 11 presents a diagram of the water-cooling system for the nozzles. During the blowdown cycle, water from the supply tank is forced through the water-cooling system at 300 lb/sq in. by applying air pressure to the top of the supply tank. Approximately 80 gal/min are forced through the cooling passage of the nozzle. At all other times, water is pumped through the nozzle at 60 lb/sq in. and through the closed circulating system. The water is treated with a mixture of sodium bichromate and sodium polyphosphate to retard rust and

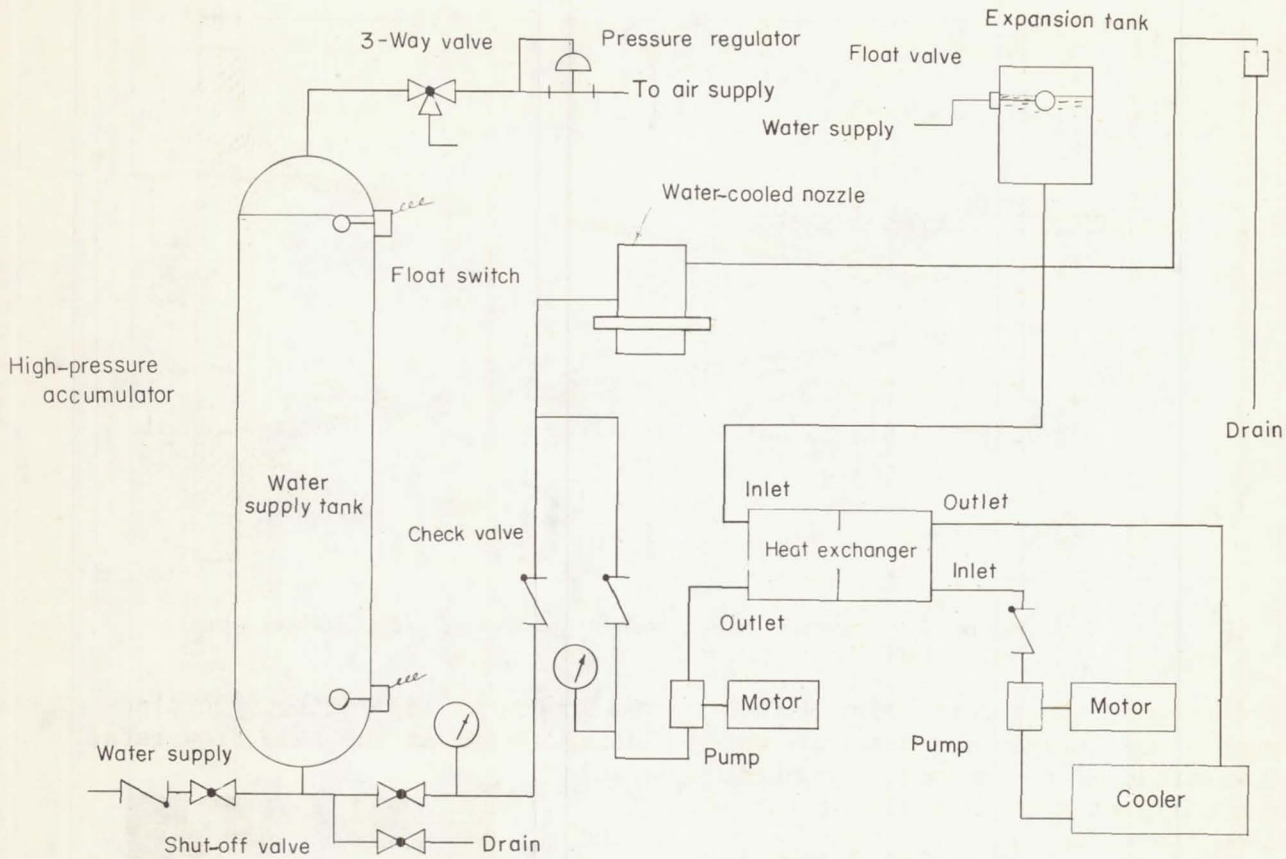


Figure 11.- Diagram of nozzle water-cooling system for 11-inch ceramic-heated tunnel.

scale formation. During the firing cycle, the closed water system is maintained at 120° F by the heat exchanger to prevent condensation of combustion products on the inside of the nozzle.

This type of nozzle has been successfully used for several hundred tests and has proved adequate up to stagnation conditions of approximately 4,050° R and 1,200 lb/sq in. Long-term rust and corrosion are still a problem; however, construction of the nozzles from stainless steel does not appear to be practical because of its lower thermal conductivity.

Mach 6 nozzle.- Figure 12 presents a diagram, and figure 13, a photograph of the Mach 6 nozzle. Construction of this nozzle is identical to the Mach 4 nozzle

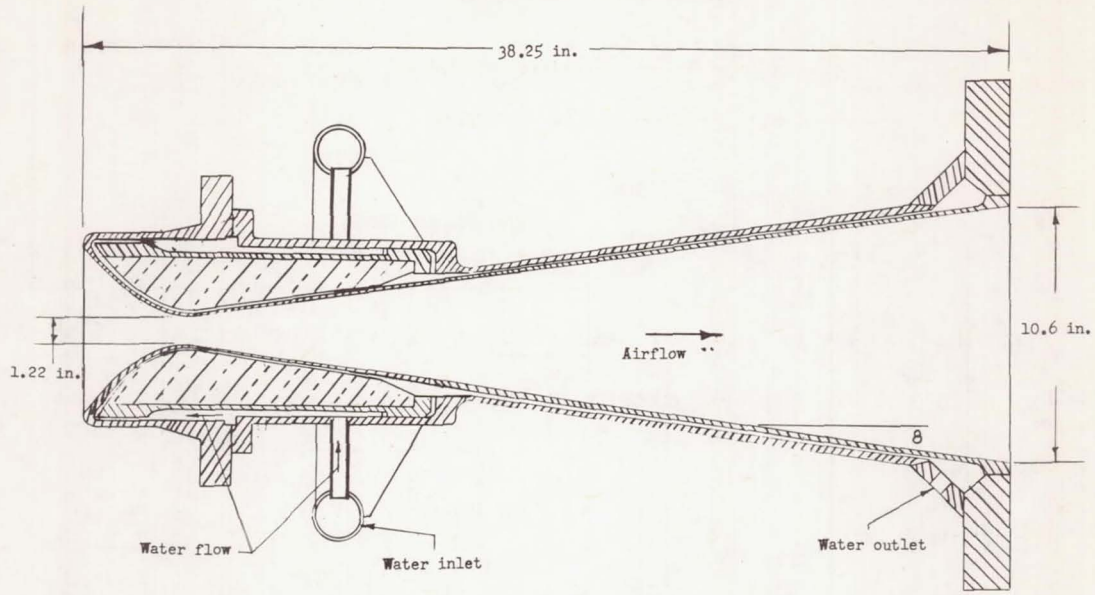


Figure 12.- Diagram of Mach 6 nozzle. Dimensions are in inches.

upstream of the throat. The Mach 6 nozzle mounts on the facility in place of the Mach 4 nozzle and uses the same water-cooling system at the same flow rates. Downstream of the throat, the airflow expands conically at a total angle of 15° and exits from the nozzle into the test section at the 10.6-inch-diameter location. The flow continues into the diffuser, where pressure is recovered, and then exhausts to the atmosphere. Performance and operational parameters for the Mach 6 nozzle and diffuser system are presented in the section entitled "Performance of Facilities." Heat-transfer considerations upstream of the throat of the Mach 6 nozzle are identical to the Mach 4 nozzle.

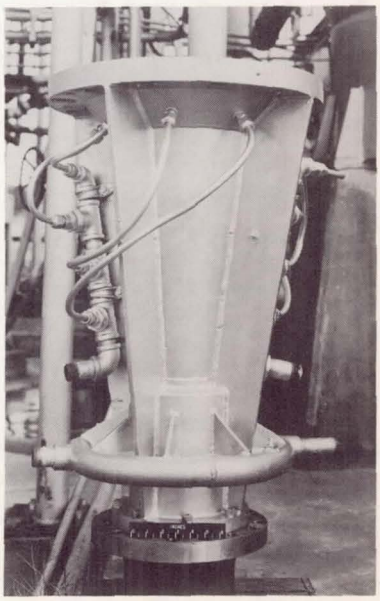

L-61-5760
Figure 13.- Photograph of Mach 6 nozzle.

Nozzle heat transfer.- The requirements for the design of the nozzle are that it produce a uniform supersonic flow with a minimum heat loss, withstand the pressure and thermal stresses imposed on it, and be resistant to oxidation and erosion in order to maintain its contour. Two methods appeared practical for cooling the nozzle, that is, film cooling and conduction cooling with a liquid-cooled wall. The second

method was considered the more desirable approach inasmuch as additional mass would not be added to the flow.

The principal stresses in the nozzle are due to the thermal gradients through the wall and the hoop stress due to pressure forces. The thermal stresses in the throat can be approximated by the equation for a thin-wall cylinder (ref. 18).

$$\sigma_t = \frac{\eta \epsilon \Delta T}{2(1 - \mu)}$$

where

$\Delta T$ temperature difference between inside and outside surface of wall

$\eta$ coefficient of thermal expansion

$\epsilon$ modulus of elasticity

$\mu$ Poisson's ratio

Thermal stress is proportional to the temperature gradient $\Delta T$ through the wall and, therefore, to the heat flux through the wall. Neglecting longitudinal conduction along the nozzle wall, the heat flux is the same from the gas to the wall, through the wall, and from the wall to the water as expressed by the equation

$$q = h_g\left(T_{aw} - T_{w,hot}\right) = \frac{k}{t}\left(T_{w,hot} - T_{w,cold}\right) = h_L\left(T_{w,cold} - T_{water}\right)$$

Analytical design of a nozzle therefore requires determination of $h_g$ in order to determine the temperature through the wall on which the thermal stress depends.

Previous experience with liquid-cooled conductive wall nozzles was confined almost entirely to rocket nozzles. A study was therefore made of the temperature gradients, film coefficients, and thermal and pressure stresses involved in designing a nozzle for $4{,}000^\circ$ R air at high pressure. Concurrently a water-cooled nozzle was built and used successfully on the facility described in reference 1.

During design work on the present facility, theoretical predictions gave a wide variation of results for nozzle-throat heat transfer. Because of the uncertainty as to what the actual throat heat transfer would be, a nozzle similar in design to that used in reference 1 was built and tested with the present facility at successively higher temperatures and pressures, with careful examination for indications of excessive thermal stress after each run. No indication of thermal-stress failure was evident when the nozzle was operated at a stagnation pressure of 815 lb/sq in. absolute and a stagnation temperature of $4{,}000^\circ$ R.

Because more information was desired concerning nozzle heat transfer, it was decided to measure heat transfer in an experimental nozzle over the proposed range

of operating conditions. In order to measure heat transfer, inlet and exit water temperatures were measured with thermocouples, and a thermocouple was spotwelded on the back wall of the throat of the nozzle and another, 2 inches downstream of the throat. Five tests were made with nominal conditions of stagnation pressures of 815 to 1,200 lb/sq in. and stagnation temperatures of 2,510° R to 4,110° R, the results of which are presented in table I.

TABLE I.- MACH 4 NOZZLE HEAT-TRANSFER TEST INFORMATION

| Run | Stagnation pressure, lb/sq in. | Stagnation temp., °R | Cooling water inlet temp., °R | Cooling water temp. rise, °R | Cooling water flow rate, gal/min | Cold wall at throat, °R | Cold wall 2 in. downstream of throat, °R |
|---|---|---|---|---|---|---|---|
| 1 | 815 | 2,520 | 524 | 9.9 | 83.6 | 620 | 584 |
| 2 | 1,200 | 2,510 | 526 | 11.6 | 83.6 | 634 | 608 |
| 3 | 1,200 | 3,210 | 535 | 15.7 | 83.6 | 670 | 637 |
| 4 | 1,200 | 4,010 | 537 | 22.6 | 83.6 | 739 | 680 |
| 5 | 815 | 3,260 | 530 | 14.7 | 83.6 | 639 | 614 |

The rate of heat transfer through the wall was determined from the experimental data by use of the equation

$$q = h_L\left(T_{w,cold} - T_{water}\right)$$

The water heat-transfer coefficient $h_L$ was determined by the methods of reference 13 for turbulent flow in concentric annular passages by the equation

$$h_l = \frac{0.023R^{0.8}N_{Pr,b}^{1/3}}{D_e}\left(\frac{\nu_b}{\nu_w}\right)^{0.14}k_b$$

where $D_e = \frac{4A}{P}$, effective diameter of cooling passage

A cross-sectional area, $ft^2$

P wetted perimeter

k thermal conductivity of liquid

R dimensionless Reynolds number

$N_{Pr}$ coolant Prandtl number

k thermal conductivity of the liquid

Subscripts:

b bulk water conditions

l liquid

g gas

w wall conditions

The nozzle throat heat-transfer coefficient was then determined from

$$h_g = \frac{q}{T_{aw} - T_{w,hot}}$$

$$= \frac{q}{T_{aw} - T_{w,cold} + \frac{q}{k/t}}$$

where subscript aw is adiabatic wall. A turbulent recovery factor of $N_{Pr}^{1/3} = 0.88$ was used in computing $T_{aw}$. Conductivity of the T-1 steel of 240 Btu-in./sq ft-hr-$^{o}$F for the nozzle wall of 0.062-inch thickness was used in the calculations. The accuracy in determining the heat transfer is dependent on the accuracy of the assumptions used in calculating water heat-transfer coefficient and the assumption of $T_{aw}$.

Figure 14 presents the values of gas boundary-layer heat transfer derived from the above tests compared with theoretical flat-plate values for laminar and turbulent flow at nozzle-throat conditions calculated by methods of Van Driest (refs. 19 and 20). As shown by this comparison, the heat transfer measured at the throat of the nozzle was less than that calculated for turbulent flow but was considerably above the values for laminar flow.

The nozzle for the facility described herein has been used several hundred times at pressures up to a maximum of 1,200 lb/sq in. absolute and up to 4,000$^{o}$ R without signs of thermal-stress failure. Operation has been limited to these conditions inasmuch as calculations from the preceding data indicate that hot metal wall temperatures approach a limiting condition of 1,700$^{o}$ R which was chosen on the basis of thermal stress and oxidation considerations.

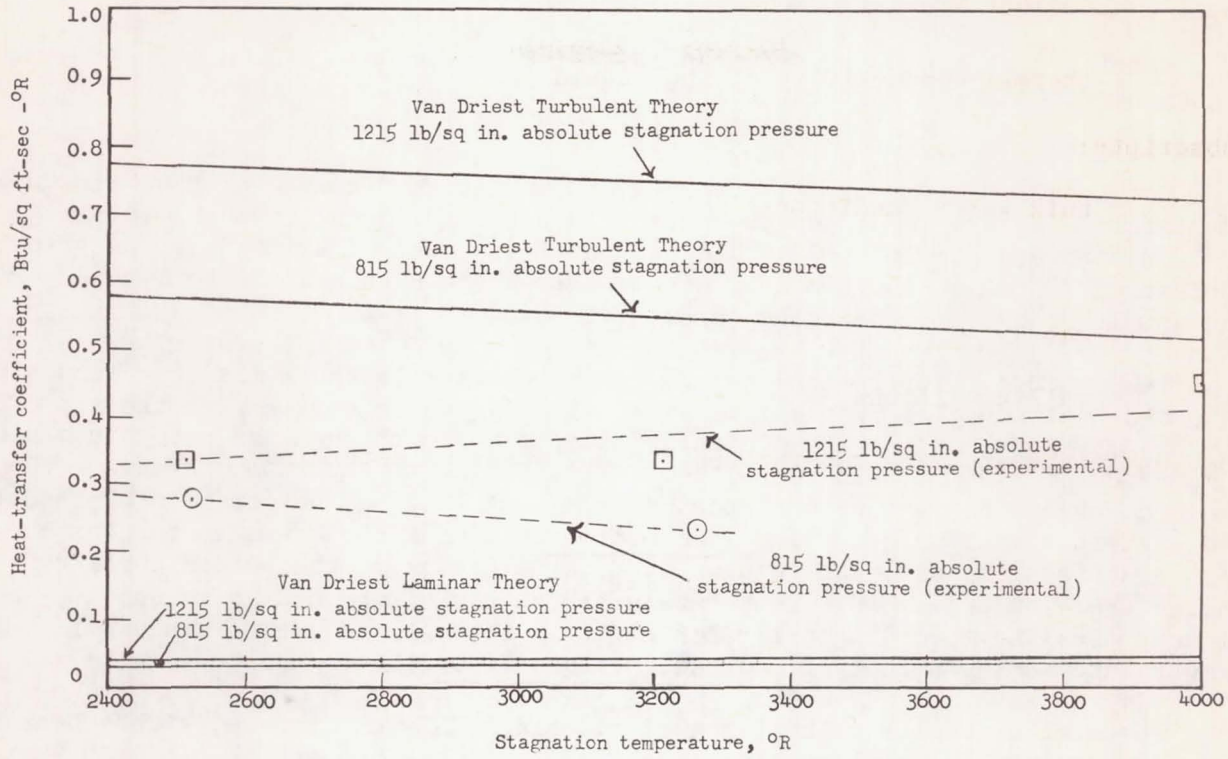


Figure 14.- Gas boundary-layer heat-transfer coefficient at throat as a function of stagnation temperature.

Table II presents a tabulation of the average temperature drop of heated air in passing through the Mach 4 nozzle, calculated from information listed in table I. It is indicated that not more than 4 percent of the total enthalpy of the airstream is absorbed by the water-cooled nozzle. The decrement of enthalpy in the flow resulting from this removal of heat is primarily in the boundary layer.

TABLE II.- TEMPERATURE DROP OF AIR PASSING THROUGH MACH 4 NOZZLE

| Run | Heat absorbed by nozzle, Btu/sec | Airflow rate, lb/sec | Computed stagnation temp. drop of air, °R |
|---|---|---|---|
| 1 | 115.5 | 10.56 | 40.7 |
| 2 | 135.0 | 14.83 | 34.5 |
| 3 | 182.9 | 13.52 | 49.3 |
| 4 | 263.0 | 11.55 | 78.5 |
| 5 | 171.1 | 8.72 | 71.5 |

## Operation of Apparatus

Heating and test cycle.- The operation of the ceramic-heated jet or tunnel system consists of two cycles: first, the heating cycle and second, the blowdown cycle.

During the heating cycle, products of combustion from the propane-air-oxygen burner (fig. 2) are forced by pressure of about 1 lb/sq in. from the settling chamber downward through the pebble bed until the desired temperature distribution is reached. Some of the products of combustion are also allowed to escape through the nozzle in order to heat the ceramics leading to it.

Temperature distribution through the pebble bed is controlled by combustion rate and heating rate. For a typical heating cycle, temperature at the top of the bed may be 4,500° R with decreasing temperatures through the bed to a maximum temperature of 1,500° R at the bottom. Maintaining a temperature gradient through the bed serves the purpose of imposing the least load on the ceramics exposed to the highest temperatures, allows the bottom retaining structure to be constructed of conventional metals, and reduces the thermal shock on the bottom ceramics during the blowdown cycle. Temperature at the top of the bed is measured by means of an optical or recording pyrometer sighting through the quartz window (fig. 2). Temperature at the bottom of the bed is measured by thermocouples.

The heat exchanger is kept hot at all times when not in use, with a heating rate of 500,000 Btu/hr which maintains the top of the bed at about 3,000° R except when it is necessary to cool it down for repairs. Heating the bed from a cold start requires approximately 24 hours, while reheating after a blowdown cycle requires from 1 to 3 hours.

After the pebble bed and surrounding brickwork are heated to the desired temperature distribution for a test run, the burner is closed off and the heat exchanger is ready for the blowdown cycle.

For the blowdown cycle, air is passed upward through the pebble bed and exhausted through the nozzle. The airflow rate into the bed is controlled during the pressurization cycle at a rate which does not allow the pressure differential through the bed to exceed 75 percent of the differential required to lift the bed. Pressure is increased until the desired stagnation pressure is reached after which the airflow rate is controlled to maintain a constant stagnation pressure. Pressurization to 800 lb/sq in. requires approximately 45 seconds. Running time is generally limited to 60 seconds but can be extended to 120 seconds with a greater total temperature drop. After the test, approximately 90 seconds are required for the pressure vessel to bleed down through the water-cooled nozzle.

Model insertions devices and model sizes.- Whenever the facility is used as a Mach 4 free jet, either the single model support system (fig. 15) or the indexing model support system (fig. 16) is used to insert the model into the jet at the control of the operator, when the desired stagnation pressure is reached. The indexing model support system is used to test up to four consecutive models during a single blowdown cycle, and has proved valuable in testing a large number

of materials specimens. Model movement in and out of the jet can be controlled manually or by a preset programmer system.

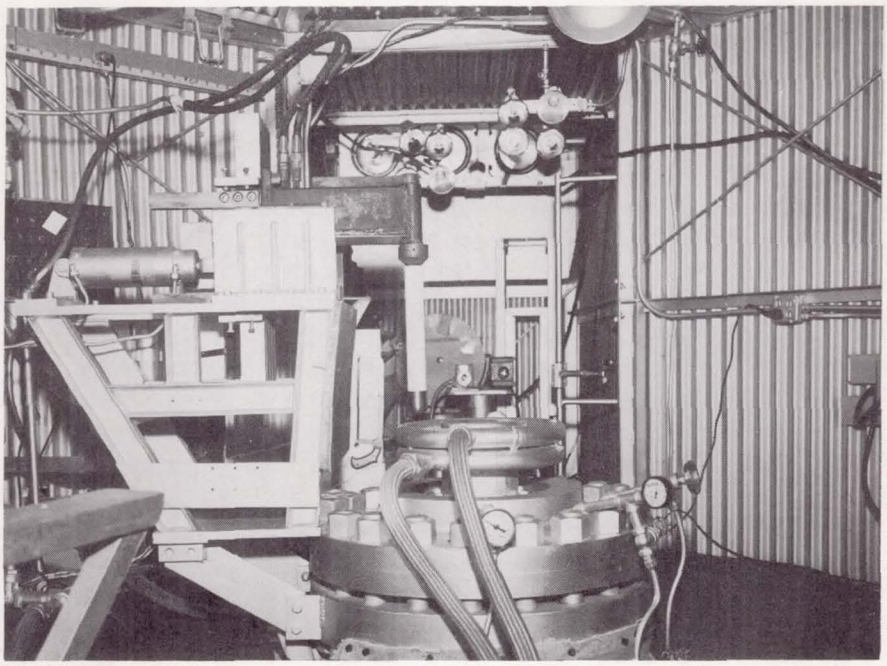

Figure 15.- Photograph of Mach 4 test section. L-61-7905

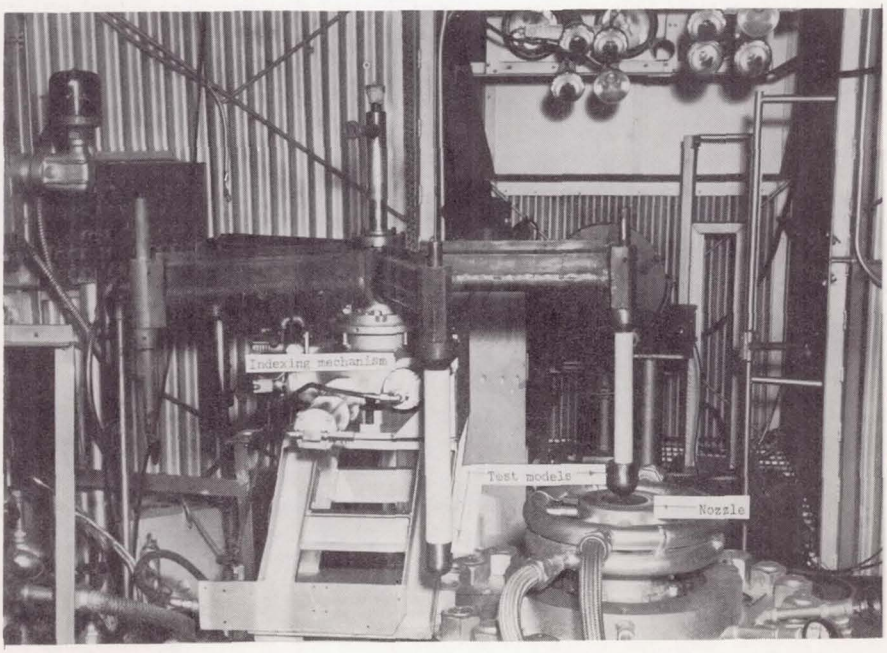


L-61-8383

Figure 16.- Photograph of indexing model-support system for Mach 4 ceramic-heated jet facility.

The model support system for the 11-inch Mach 6 tunnel system can be seen in figures 3 and 17. The model support system is attached to a carriage mounted on a track. The carriage is powered by a pneumatic cylinder to insert or remove the model from the jet. The box containing the carriage is enclosed and sealed during a test, since the test section operates at a free-stream pressure of less than 0.5 lb/sq in. after the tunnel is started. The model is protected from the heat of the jet, before and after the test, by a door between the test section and the box containing the model support system.

Instrumentation.- Tunnel stagnation pressure and pressure drop across the pebble bed are observed on visual gages and are recorded on chart recorders. The temperature of the top of the pebble bed is measured with an optical pyrometer before and after each test and is measured with a recording pyrometer during tests to determine the rate of change of temperature with time. These measurements indicate that the temperature of the top of the pebble bed drops about $5^{\circ}$ F/sec during a blowdown cycle. Measurements with thermocouple probes at the exit of the water-cooled nozzle during a test indicate that for tests at about $2,500^{\circ}$ R, the air stagnation temperature is about equal to the average of the "before-blowdown" and "after-blowdown" temperatures at the top of the bed and for temperatures near $4,000^{\circ}$ R is from $100^{\circ}$ to $200^{\circ}$ F below average temperature at the top of the bed.

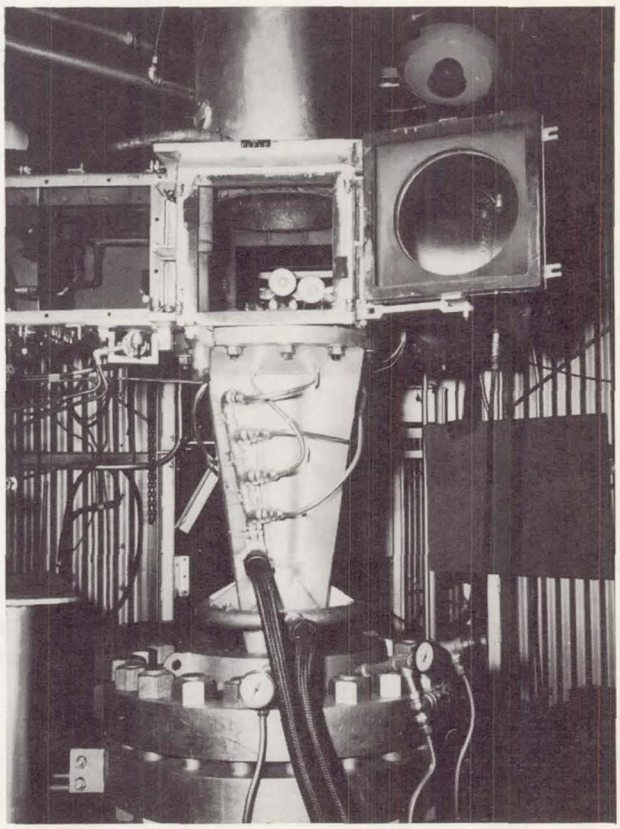

L-61-5400

Figure 17.- Photograph of Mach 6 nozzle and test section for the 11-inch ceramic-heated tunnel.

Tunnel-pressure data and model temperature and pressure data obtained from thermocouples and pressure transducers are recorded on two 18-channel recording oscillographs. The models may be observed during a test by a remote television viewing system or, in the case of the Mach 4 nozzle, by a periscope. Motion-picture cameras are also used for obtaining visual data during a test. A shadowgraph system is used with both the Mach 4 and the Mach 6 test sections to obtain pictures of the tunnel flow.

## Performance of Facilities

The two nozzle systems provided with the heat exchanger give a wide range of enviromental capabilities. The facilities have been used in many types of high-temperature research, materials testing, heat-transfer studies, and aerodynamic

testing. The usefulness of this facility for refined aerodynamic testing is at present limited by erosion of model surfaces which results from contamination of the airstream by zirconia dust particles.

Mach 4 nozzle.- This nozzle provides a free jet 4 inches in diameter at the exit suitable for testing aerodynamic and materials models at stagnation temperatures from 2,000° to 4,000° R, with stagnation pressures from 400 lb/sq in. to as high as 1,200 lb/sq in.; however, the minimum pressure used is 800 lb/sq in. because of nozzle shock intersection. A shadowgraph of the flow from this nozzle operating at a stagnation pressure of 815 lb/sq in. absolute is presented in figure 18. The boundary shock from this nozzle, which is operated in an overexpanded condition because of pressure limitation, produced a high local heating rate where the shock waves intersect any surface; therefore, for tests requiring uniform flow conditions, model diameters are generally limited to 2 inches to keep within the shock boundaries.

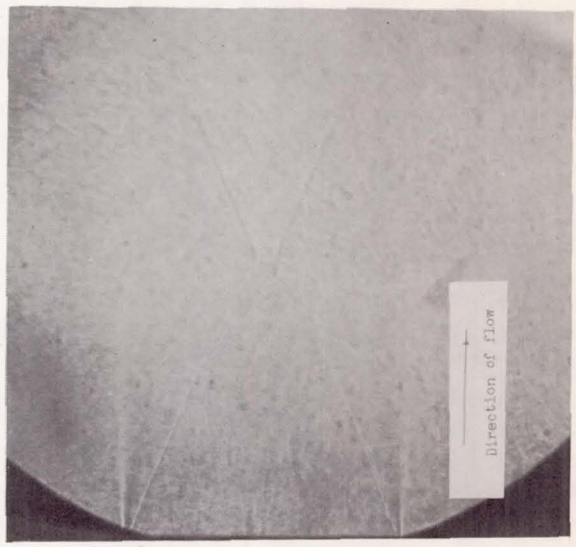


L-62-7031

Figure 18.- Shadowgraph of flow from Mach 4 nozzle operated at stagnation pressure of 815 lb/sq in. absolute and stagnation temperature of 3,500° R.

Figure 19 presents a variation of calculated Mach number and velocity with stagnation temperature for the Mach 4 nozzle operating at 815 lb/sq in. absolute. Also shown as a function of stagnation temperature on the center line are measured values of Mach number derived from pitot pressure and total-temperature measurements made 1/2 inch beyond the nozzle exit. Calculated velocity varies from 4,400 ft/sec at 2,000° R to 6,610 ft/sec at 4,100° R, while calculated values of Mach number vary from 3.96 at 2,000° R to 3.74 at 4,100° R. Measured values of Mach number were from $1\frac{1}{2}$ to $3\frac{1}{2}$ percent higher than calculated values. Calculations were made by methods presented in reference 21 and were checked by methods presented in reference 22.

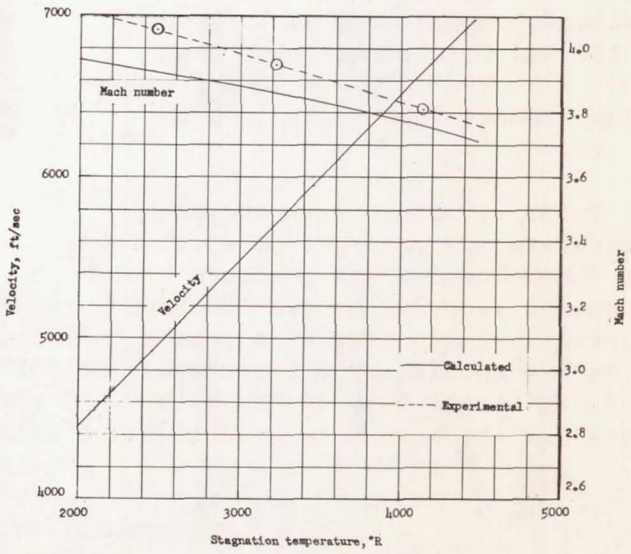


Figure 19.- Variation of Mach number and velocity with stagnation temperature for Mach 4 nozzle.

Figure 20 presents variation of calculated values of free-stream static pressure and temperature with stagnation temperature for the Mach 4 nozzle. Free-stream pressure varies from 6.8 lb/sq in. absolute at 2,000° R to 6.95 lb/sq in. absolute at 4,100° R while free-stream temperature varies from 525° R at 2,000° R to 1,360° R at 4,100° R.

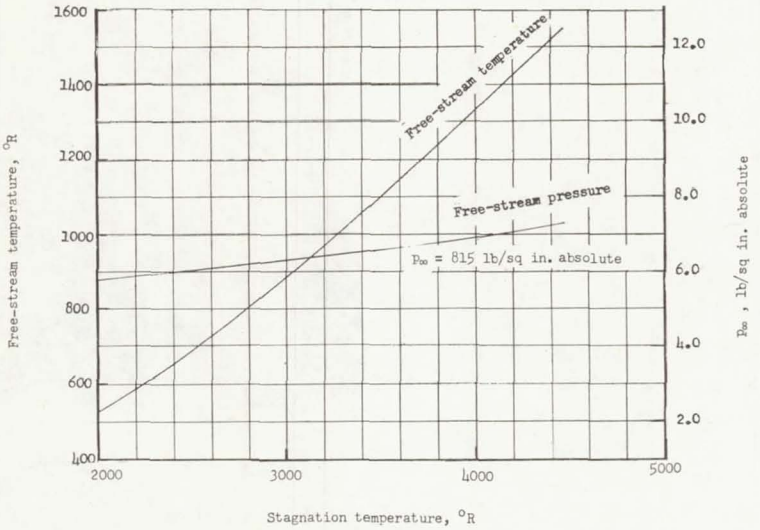


Figure 20.- Variation of free-stream pressure and temperature with stagnation temperature for Mach 4 nozzle.

Figure 21 presents the variation of calculated Reynolds number per foot with stagnation temperature. Reynolds number per foot varies from $7.76 \times 10^6$ at 2,500° R to $3.94 \times 10^6$ at 4,000° R.

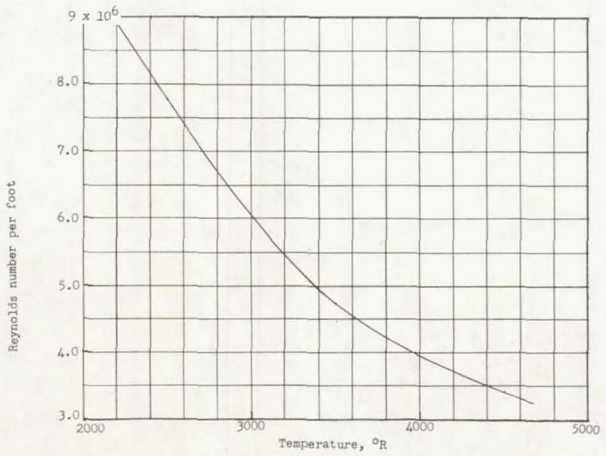


Figure 21.- Variation of free-stream Reynolds number with stagnation temperature for Mach 4 nozzle. $p_\infty$ = 815 lb/sq in. absolute.

Figure 22 presents the variation of heating parameter $h\sqrt{D}$ for the stagnation point of a hemisphere with stagnation temperature for the Mach 4 nozzle as calculated by methods presented in reference 23.

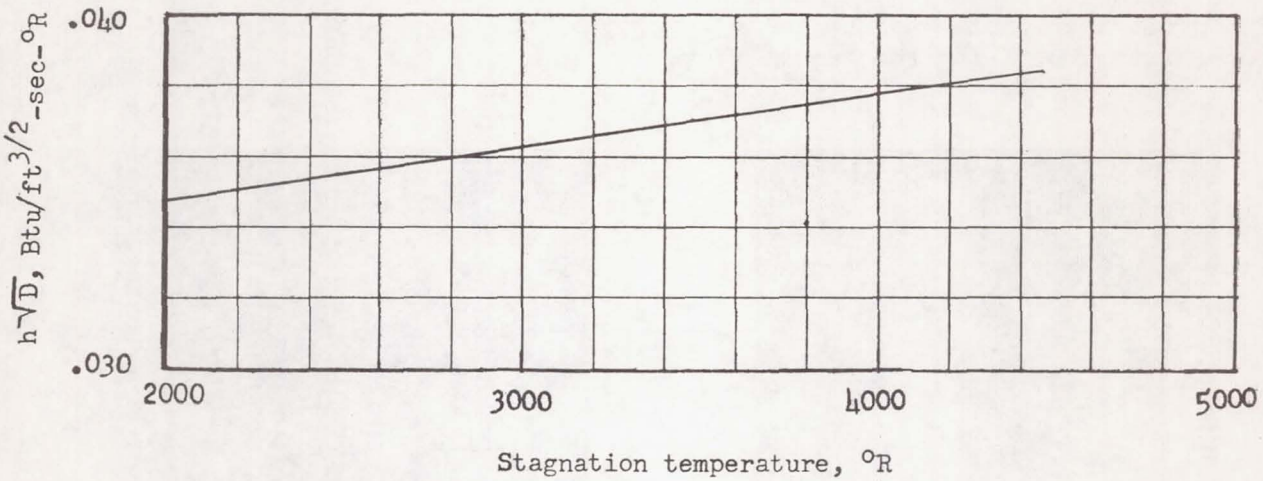


Figure 22.- Variation of heating rate for stagnation-point heating of hemispheric model with stagnation temperature for Mach 4 nozzle. $p_{\infty}$ = 815 lb/sq in. absolute.

Mach 6 ceramic-heated nozzle.- The Mach 6 nozzle which has a 10.6-inch exit diameter is suitable for aerodynamic, heat-transfer, and materials testing. The nozzle-diffuser system is designed to operate at stagnation pressures from 815 to 1,215 lb/sq in. and stagnation temperatures from 2,000° R to 4,100° R. Table III presents the model sizes that have been tested in the facility. Axisymmetrical flat-face models up to $2\frac{1}{2}$ inches in diameter and hemispherical models up to 4 inches in diameter can be tested at 1,200 lb/sq in. stagnation pressure without blocking the tunnel flow.

TABLE III.- MODEL BLOCKAGE INFORMATION

| Model | | Blockage, percent | Stagnation pressure, lb/sq in. absolute | Results |
|---|---|---|---|---|
| 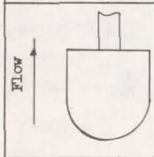  | 2-in. hemisphere cylinder | 3.56 | 815 - 1,215 | Ran satisfactorily |
| | 3-in. hemisphere cylinder | 8.64 | 815 - 1,215 | Ran satisfactorily |
| | 4-in. hemisphere cylinder | 14.28 | 815 - 1,015 | Blocked flow<br>Ran satisfactorily |
| 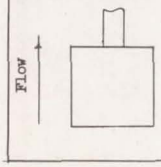  | 2-in. flat-face cylinder | 3.56 | 815 - 1,215 | Ran satisfactorily |
| | $2\frac{1}{2}$-in. flat-face cylinder | 5.57 | 815 - 1,215 | Ran satisfactorily |
| | 3-in. flat-face cylinder | 8.64 | 815 - 1,215 | Blocked flow |

Figure 23 presents shadowgraphs of 2-, 3-, and 4-inch hemispherical models and a 3-inch-diameter flat-face model with beveled edges in the Mach 6 flow. The tunnel permits axisymmetrical models which do not choke the tunnel flow to be tested without boundary-shock intersection. Irregularly shaped configurations with cross-sectional areas up to 14 percent of the nozzle-exit area have been tested without choking the tunnel flow.

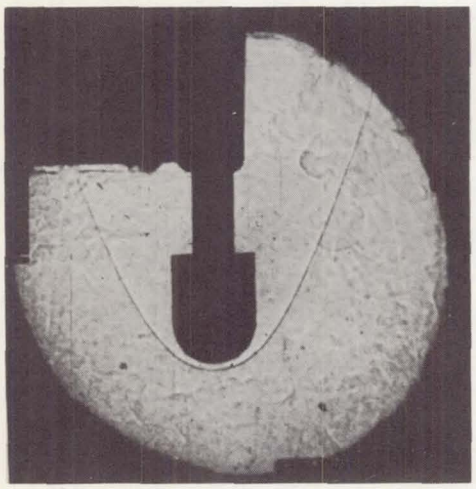

2-inch hemisphere

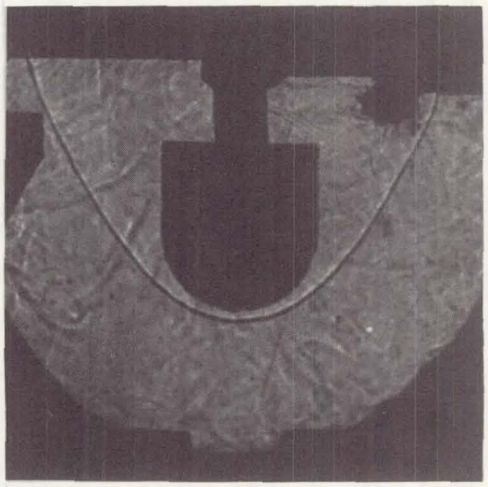

3-inch hemisphere

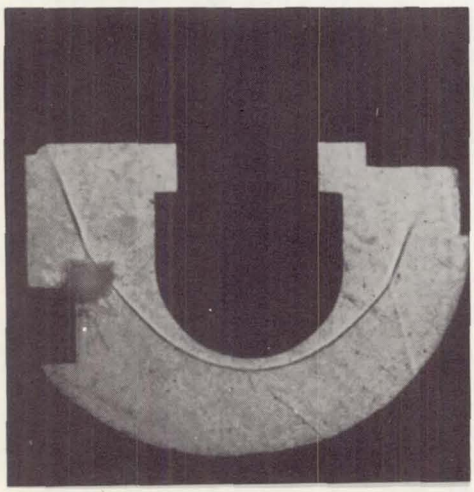

4-inch hemisphere

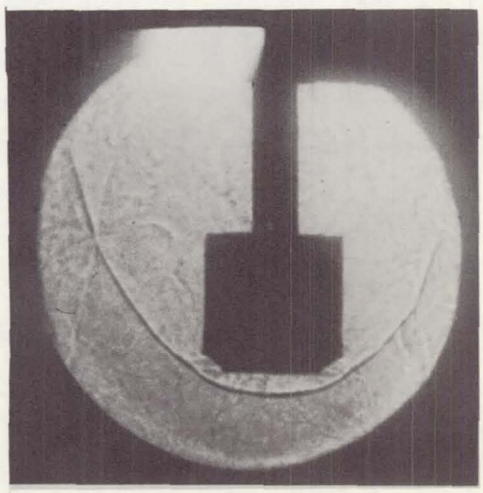

3-inch beveled cylinder

L-62-7032

Figure 23.- Shadowgraphs of flow from Mach 6 nozzle.

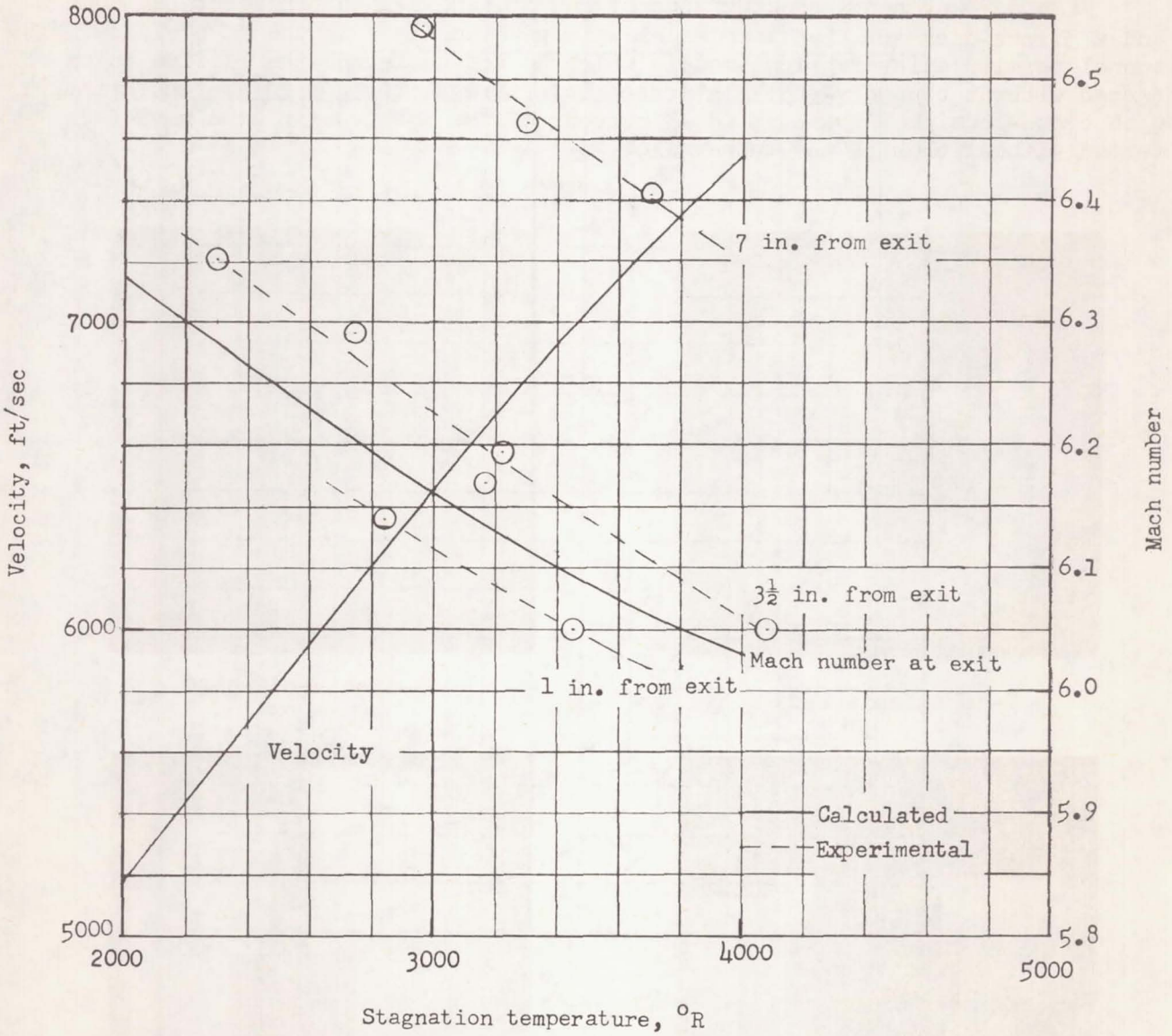


Figure 24.- Mach number and velocity as a function of stagnation temperature for Mach 6 nozzle.

Figure 24 presents calculated velocity and Mach number as a function of stagnation temperature. Experimentally determined values of Mach number are also presented as a function of distance from the exit of the nozzle. Flow from the conical nozzle continues to expand and increase in Mach number beyond the nozzle exit.

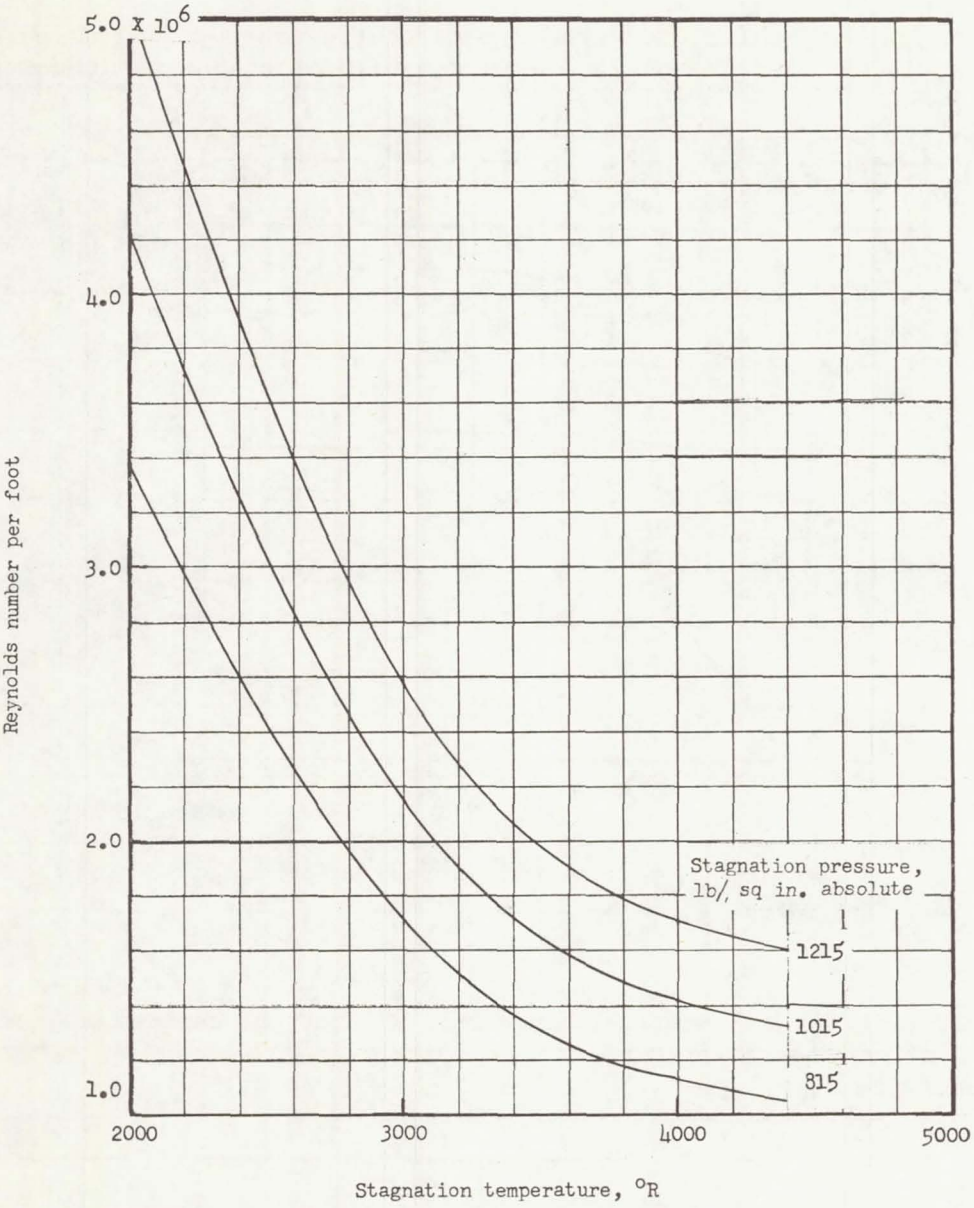


Figure 25.- Variation of free-stream Reynolds number per foot as a function of stagnation temperature for Mach 6 nozzle.

Figure 25 presents calculated Reynolds number as a function of stagnation temperature for 815, 1,015, and 1,215 lb/sq in. stagnation pressures. Reynolds number varies from $5 \times 10^6$ at 1,215 lb/sq in. absolute and 2,000° R to $1.12 \times 10^6$ at 815 lb/sq in. absolute and 4,000° R at distances 1 inch from the exit on the center line.

Figure 26 presents calculated free-stream static pressure and temperature (1 inch beyond the exit of the nozzle) as a function of stagnation temperature.

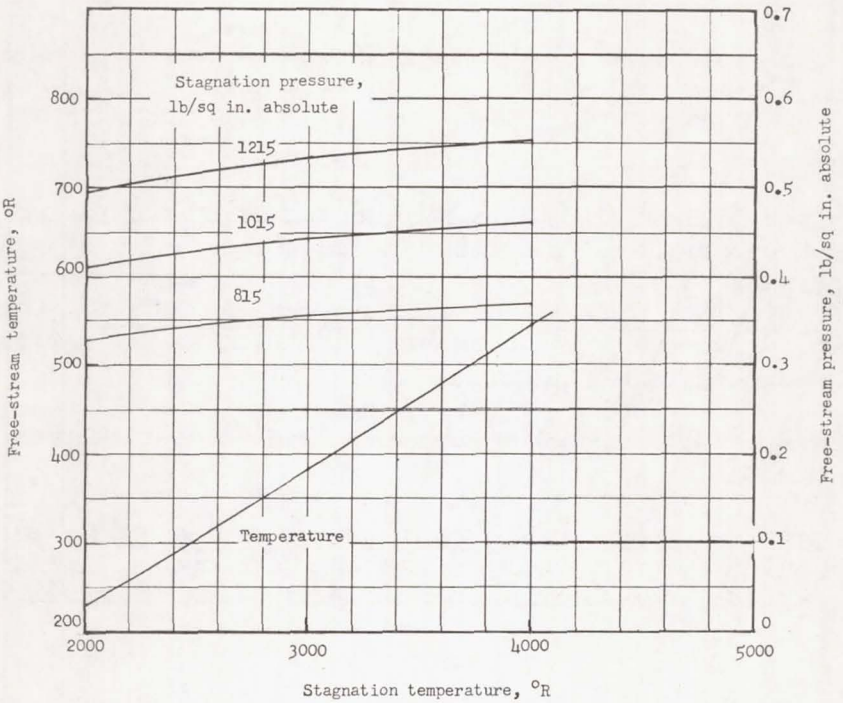


Figure 26.- Free-stream static pressure and static temperature as a function of stagnation temperature for Mach 6 nozzle.

Figure 27 presents the heating parameter $h\sqrt{D}$ at the stagnation point of a hemisphere as a function of stagnation temperature as calculated by methods presented in reference 23.

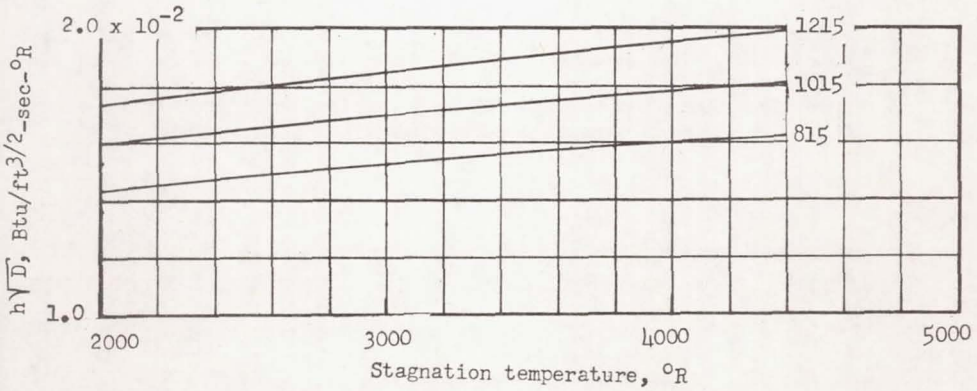


Figure 27.- Variation of heating rate at stagnation point of hemisphere as a function of stagnation temperature for Mach 6 nozzle.

## CONCLUDING REMARKS

The results of this program to develop high-temperature research facilities utilizing a ceramic heat exchanger may be concluded as follows:

1. The concepts applied in the development of a $4,500^{\circ}$ R ceramic heat exchanger for wind-tunnel application have proved practical. A facility comprising a $4,500^{\circ}$ heat exchanger has been successfully designed, constructed, and used for testing.

2. A Mach 4 free jet and an 11-inch Mach 6 tunnel system have been developed to operate from the ceramic heat exchanger for materials and heat-transfer research and aerodynamic testing. The zirconia heat exchanger provides a practical means for heating air to $4,000^{\circ}$ R for research facilities. Contamination of the heated air by small amounts of zirconia dust limits the usefulness of the facility for refined materials testing.

3. Water-cooled nozzles have been developed and successfully employed on the ceramic-heated tunnels.

4. A simple premixed propane-air-oxygen burner system which is capable of heating of the ceramics to over $4,500^{\circ}$ R has been developed. The system provides clean, easily controllable combustion over the entire operating range.

Langley Research Center,
National Aeronautics and Space Administration,
Langley Station, Hampton, Va., October 16, 1962.

## REFERENCES


1. Perry, John H., ed.: Chemical Engineers' Handbook. Third ed., McGraw-Hill Book Co., Inc., 1950.

2. Norton, C. L., Jr.: The Pebble Heater - A New Transfer Apparatus. Jour. American Ceramic Soc., vol. 29, no. 7, July 1946, pp. 187-193.

3. Batchelder, H. R., and Ingols, H. A.: Performance of a Pebble Heater Type Steam Superheater. Rep. of Invest. 4781, Bur. Mines, U.S. Dept. Interior, Mar. 1951.

4. Buehl, R. C., Morris, J. P., and Riott, J. P.: Pebble Stoves for Heating Gases to High Temperatures. Rep. of Invest. 4949, Bur. Mines, U.S. Dept. Interior, Mar. 1953.

5. Liu, Tung-Sheng, Sun, Ernst J. C., and Knutson, Robert K.: The Design and Performance of a Regenerative-Type Heater for an Intermittent Supersonic Wind Tunnel. WADC Tech. Rep. 56-215, ASTIA Doc. NR AD 131020, U.S. Air Force, Nov. 1957.

6. Bloom, Martin H.: A High Temperature-Pressure Air Heater (Suitable for Intermittent Hypersonic Wind-Tunnel Operation). WADC Tech. Note 55-694, ASTIA Doc. No. AD 110725, U.S. Air Force, Nov. 1956.

7. Fields, E. M., Hopko, Russell N., Swain, Robert L., and Trout, Otto F., Jr.: Behavior of Some Materials and Shapes in Supersonic Free Jets at Stagnation Temperatures up to 4,210° F, and Descriptions of the Jets. NACA RM L57K26, 1958.

8. Hopko, Russell N., and Trout, Otto F., Jr.: Exploratory Tests of the Behavior of Several Materials in a Supersonic Air Jet at 4,000° F. NACA RM L57E24, 1957.

9. Trout, Otto F., Jr.: Experimental Investigation of Several Copper and Beryllium Hemispherical Models in Air at Stagnation Temperatures of 2,000° F to 3,600° F. NASA TM X-55, 1959.

10. Norton, F. H.: Refractories. Third ed., McGraw-Hill Book Co., Inc., 1949.

11. Campbell, I. E. (ed.): High-Temperature Technology. John Wiley & Sons, Inc., c.1956.

12. Anon.: Zirconia, Bonded Refractories. CP5.5.3, Refractories Div., Norton Co., Worcester, Mass., June 30, 1955.

13. McAdams, William H: Heat Transmission. Third ed., McGraw-Hill Book Co., Inc., 1954.

14. Hogerton, J. F., and Grass, R. C., eds.: The Reactor Handbook. Vol. 2 - Engineering. AECD - 3646. U.S. Atomic Energy Commission, May 1955.

15. Brown, George Granger, Foust, Alan Shivers, et al.: Unit Operations. John Wiley & Sons, Inc., c.1950.

16. Lewis Propulsion Chemistry Division (Henry C. Barnett and Robert R. Hibbard, eds.): Basic Considerations in the Combustion of Hydrocarbon Fuels With Air. NACA Rep. 1300, 1957.

17. Bailey, A., and Wood, S. A.: The Conversion of the Stanton 3-Inch High-Speed Wind Tunnel to the Open Jet Type. Proc. Inst. Mech. Eng. (London), vol. 135, Jan.-May 1937, pp. 462-466.

18. Timoshenko, S.: Strength of Materials. Part II - Advanced Theory and Problems. Third ed., D. Van Norstrand Co., Inc., c.1956.

19. Van Driest, E. R.: The Turbulent Boundary Layer With Variable Prandtl Number. Rep. No. AL-1914, North American Aviation, Inc., Apr. 2, 1954.

20. Van Driest, E. R.: Investigation of Laminary Boundary Layer in Compressible Fluids Using the Crocco Method. NACA TN 2597, 1952.

21. Ames Research Staff: Equations, Tables, and Charts for Compressible Flow. NACA Rep. 1135, 1953. (Supersedes NACA TN 1428.)

22. Erickson, Wayne D., and Creekmore, Helen S.: A Study of Equilibrium Real-Gas Effects in Hypersonic Air Nozzles, Including Charts of Thermodynamic Properties for Equilibrium Air. NASA TN D-231, 1960.

23. Sibulkin, M.: Heat Transfer Near the Forward Stagnation Point of a Body of Revolution. Jour. Aero. Sci. (Readers' Forum), vol. 19, no. 8, Aug. 1952, pp. 570-571.